PCCP

Accepted Manuscript

ROYAL SOCIETY OF CHEMISTRY

www.rsc.org/pccp

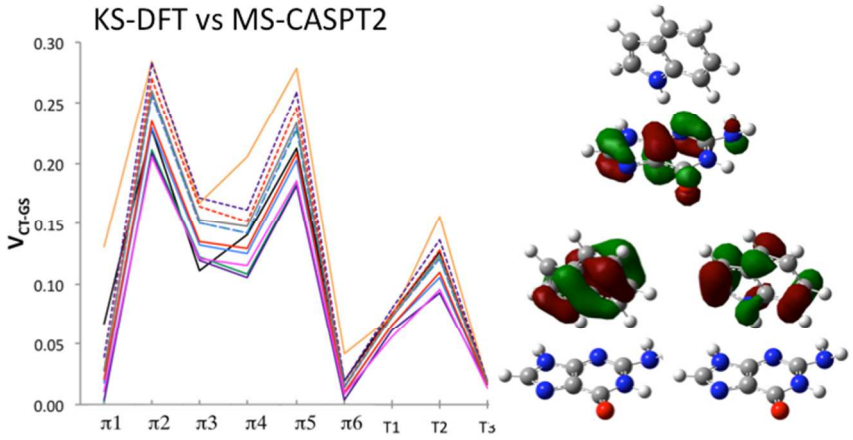

TOC

The electron transfer parameters for the 3-state G•••Ind system can be obtained with an efficient Kohn-Sham orbital based scheme.

On the performance of the Kohn-Sham orbital approach in the calculation of electron transfer parameters. Three state model

C. Butchosa,[§,¶] S. Simon,[§*] L. Blancafort,[§] A. A. Voityuk[§,‡*]

[§]*Institut de Química Computacional i Catàlisi (IQCC) and Departament de Química, Universitat de Girona, Campus de Montilivi, 17071 Girona, Spain.* [¶]*Department of Chemistry, University College London, 20 Gordon Street, London WC1H 0AJ, United Kingdom.* [‡]*Institució Catalana de Recerca i Estudis Avançats (ICREA), Barcelona, Spain.*

*To whom correspondence should be addressed. E-mail: *silvia.simon@udg.edu* and *alexander.voityuk@icrea.cat*

Abstract. We have tested the performance of the Kohn-Sham orbital approach to obtain the electronic coupling and the energetics for hole transfer (HT) in the guanine-indole pair, treated with a three-state model. The parameters are derived from the simple DFT calculations with 10 different functionals, and compared with benchmark MS-CASPT2 calculations. The guanine-indole pair is a simple model for HT in DNA-protein complexes, which has been postulated as a protection mechanism for DNA against oxidative damage. In this pair, the excited state of the indole radical cation has low energy (less than 0.3 eV relative to the ground state of the cation), which requires to apply very accurate quantum chemical methods and prevents the use of the standard 2-state treatment and requires to invoke a 3-state model. The Kohn-Sham orbital approach has been tested on six π stacked and three T-shaped conformers. It is shown to provide quite accurate results for all ten tested functionals, compared to the reference MS-CASPT2 values. The best performance is found for the long-range corrected CAM-B3LYP functional. Our results suggest that the Kohn-Sham orbital method can be used to estimate excited state

properties of radical cation systems studied by transient spectroscopy. Because of its accuracy and its low computational cost, the approach allows one to calculate relatively large models and to account for the effects of conformational dynamics on HT between DNA and protein environment.

Introduction

Hole transfer (HT), i.e. the migration of radical cation states, plays a fundamental role in many biological processes and has received great attention from experimentalists and theoreticians in the last decades.[1-5] The most prominent examples include the migration of holes through DNA π stacks,[3] the repair of damaged DNA by photolyases,[6] or the migration of holes from DNA to a neighboring cofactor or protein amino acid residue.[7-14] In recent papers,[15-18] we have turned our attention to the latter case, namely HT in DNA-protein complexes. This process is believed to occur, among others, in the complexes formed by DNA in nucleosome core particles and has been postulated as a mechanism that protects genomic DNA from the oxidative damage caused by other cell components or by external radiation.[8,10] Although it may have great relevance in nature, this mechanism has not received much theoretical attention up to now, and its details are still poorly understood. This has been the motivation for our interest in this subject.

In DNA, guanine (G) has the lowest ionization potential among the nucleobases and acts as a trap for the hole charge generated in the nucleobase stack. Several mechanisms have been discussed for the repair of oxidized G by proteins, including electron transfer from an aromatic amino acid[8,10] or from an ion[9] and proton coupled electron transfer.[19] Here we focus on the first case, which has been shown to occur, for example, when tryptophan residues are intercalated in DNA oligomers.[12-13] In our previous studies, we calculated diabatic parameters, site energies and electronic couplings, that determine the electron transfer rate. It was shown that the electronic interaction in the systems formed by an oxidized purine base (adenine, A, or G) and an aromatic amino acid (phenylalanine, hystidine, tyrosine or tryptophan) is strong enough to ensure effective hole transfer.[16] This is the case both for π stacked and T-shaped complexes. Similar results were found in Ref. [20], where the π stacked complexes of oxidized G with an aromatic amino acid

residue showed substantial delocalization of the charge between the two species. In further studies we also showed that electronic coupling between the purine bases is strongly conformation dependent, which highlights the importance of structural, i.e. dynamic effects on the HT process.[17-18]

The G-Ind system, which is representative of guanine-tryptophan complexes, is particularly relevant in this context. It is formed by indole (Ind), the residue of the tryptophan amino acid, and G, which are the nucleobase and amino acid residue with the lowest oxidation potentials. This model has an important difference compared with the stacked dimers formed by two nucleobases or by G and other aromatic amino acid residues.[15] The oxidized Ind^+ species has a small energy gap between its ground and first excited states, and the excited state becomes relevant for the HT because of its low energy. As a consequence, the two-state model commonly applied for thermal ET, which includes two diabatic states with the charge localized respectively on donor and acceptor, is of limited use. Instead, to describe the cation radical $[G\text{-}Ind]^+$ a three-state model should be used. It includes the ground and excited states Ind_1^+ and Ind_2^+, to which we refer further as GS (ground state) and ES (excited state), and the CT (charge transfer) state G^+ with the hole on guanine. An effective two-state treatment that accounts for these three states was recently developed.[15]

In the preceding study of the G-Ind system we used high-level MS-CASPT2 (multistate formulation of complete active space second order perturbation theory) calculations. However, this level of theory is not affordable in practice if one wants to consider the conformational flexibility of a DNA-protein aggregate and take into account the changes in the diabatic energies and electronic couplings for different conformations. Therefore, it is necessary to employ more efficient approaches to estimate these parameters, and one of our main goals is to test such an

approach for the three-state G-Ind system against the MS-CASPT2 benchmark. In fact, there is currently great interest in developing more computationally efficient approaches for the calculation of these parameters. Recent examples are the use of the self-consistent-charge density functional tight binding (SCC-DFTB) level within a coarse-grained DFT formalism,[21-22] which has been used for QM/MM simulations of fast charge transfer in DNA photolyase,[23] and the frozen density embedding formalism,[24] which provides good results with exchange-correlation functionals that contain a high percentage of exact exchange. The approach that we have benchmarked in the present work is the use of Kohn-Sham orbitals from DFT calculations on neutral systems to calculate the parameters (see for example Ref. [25]). In past work on hole and excess electron transfer in stacked nucleobase pairs we have shown that it provides reliable estimates of the parameters compared to CASPT2 or MS-CASPT2.[26-27] However, up to now the Kohn-Sham orbitals approach has been only used to describe systems within the two-state model, where the considered states correspond to a linear combination of the ground states of the donor and acceptor radical cations. In this study we show that the method can be extended by including also excited states of these species. We note that often the excitation energies of radical cations are small (less than 0.5 eV) and therefore accurate quantum-mechanical methods should be applied. In this study, we demonstrate a good performance of the simple Konh-Sham scheme in the treatment of excited states of the transient species. To this end, we test 10 different functionals for the three-state case in a set of conformers of the G-Ind pair, six π stacked and three T-shaped ones (see Figure 1 for two representative examples).

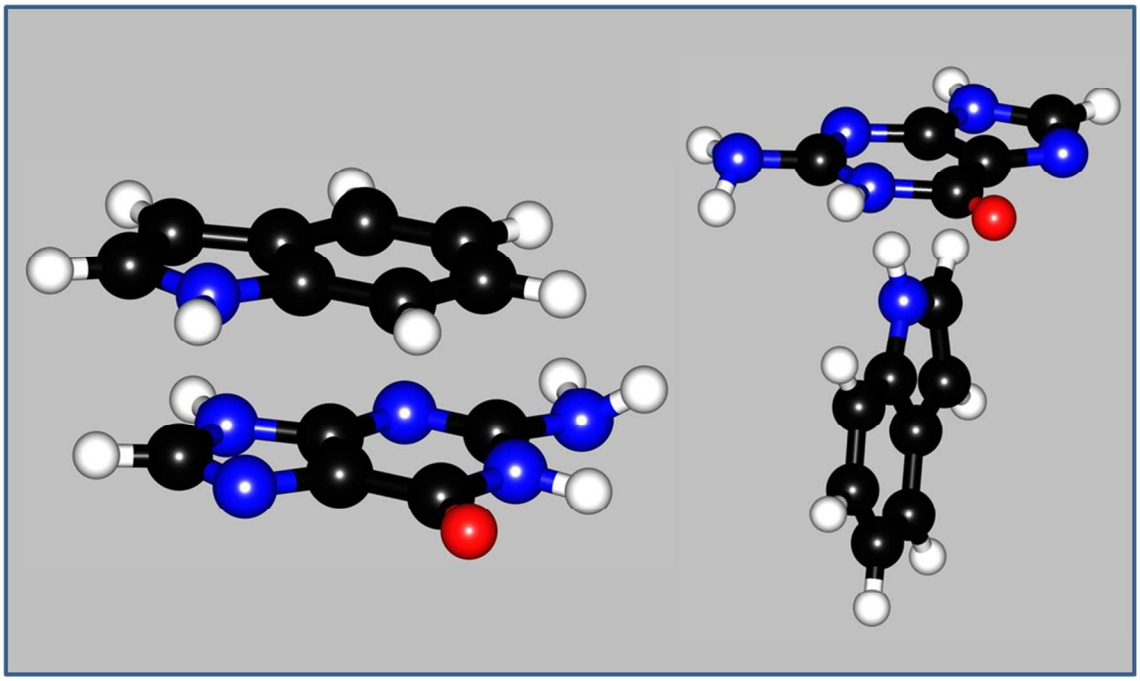

Figure 1. Representative examples of a π stacked (π2, left) and a T-shaped (T1,) conformer of the $[G\text{-}Ind]^+$ system.

Our results show that the Kohn-Sham orbitals approach provides reliable estimates of the parameters compared to those obtained from MS-CASPT2. This includes the diabatic energies of the three states and the couplings between the G localized CT state and the Ind localized GS and ES ones. The parameters depend on the conformation of the dimer, and the trends followed by the parameters at the MS-CASPT2 level are well reproduced by the Kohn-Sham based approach. Moreover, the performance for the 10 functionals of the study is similar, regardless of their different nature. Thus, the approach appears to be quite robust when computing excited state properties of the radical cation systems. Our study also provides new insights into the importance of the three-state model for HT in the G-Ind system. In particular, we find that in the T-shaped conformers the Ind^+ excited state, ES, is isoenergetic or more stable than the G^+ state, CT. Therefore, the three-state model will be particularly important for this conformation.

Computational Details

MS-CASPT2 calculations. The benchmark calculations were carried out at the MS-CASPT2 level of theory (multistate formulation of CASPT2 that accounts for the nonorthogonality of the CASPT2 wave function).[28] For the underlying complete active space self-consistent field (CASSCF) wave function we used an active space of 11 electron on 12 orbitals (6 π orbitals per molecule) and the ANO-S basis set contracted to 3s2p1d for C, N, and O, and 2s1p for hydrogen. The wave function was computed for five states, state-averaging with equal weights, and a real level shift parameter[29] of 0.2 was used for the for the CASPT2 calculations. Five states were included in the calculation to make sure that the multi-state treatment included all relevant states. The state and transition dipole moments were derived from the perturbationally modified CAS configuration interaction (PM-CASCI) wave function obtained from the MS-CASPT2 calculation. Further details on the MS-CASPT2 calculations can be found in our preceding study of the G-Ind system at this level of theory.[15]

DFT Functionals Single point DFT calculations were carried out using 10 different functionals and the 6-31G* basis set. Among the large number of available functionals, we chose two of the most widely used GGA functionals (BP86[30-31] and BLYP[30,32]) and two hybrid (B3LYP[33] and PBE0[34]) (see for instance a recent popularity poll[35]). In addition, we chose the hybrid functional of Truhlar and Zhao, M06, together with its M06-2X variation which accounts for larger HF exchange.[36] It is also well-known that common density functionals are inaccurate for charge transfer processes because long-range correlation is not treated properly.[37-40] Therefore, we have included four long-range corrected (LC) functionals in our set to test whether the calculation of the couplings is improved within the present formalism. These functionals,

which are related to the non-LC ones of our set, are LC-ωPBE,[41] CAM-B3LYP,[42] ωB97X-D[43] and LC-BLYP.[44] LC-ωPBE, LC-BLYP, ωB97X-D and CAM-B3LYP have been demonstrated to improve the description of processes related to charge transfer.

Geometries. We used a set of six π stacked conformations with a parallel arrangement of the subunits, together with three T-shaped conformations. Structures π2 and T1 are shown in Figure 1, and the remaining ones are presented in the SI, together with the Cartesian coordinates. The π stacked conformers were used in our previous study of the G-Ind system with the three-state model, and we keep the nomenclature used there. The distance between the planes of the molecules (rise parameter) is 3.38 Å. The reference structure is π1 with optimal stacking of the rings, and the remaining structures are obtained displacing the rings. Further details can be found in Ref. [15] T-shaped structures for the guanine-indole systems are extracted from Ref. [18]. They were generated with a distance between subunits of 5.38 Å, where different movement of rolling and tilting were applied. T1, T2 and T3 correspond to structures with stronger coupling. For more details see Ref. [16].

Electron-transfer parameters. The HT parameters calculated in this study are the relative diabatic energies of the states, ε, and the electronic coupling V_{DA}. These parameters appear in the rate expression for HT (k_{HT}) between a pair of donor an acceptor states, given by the Marcus equation:

$$k_{HT} = \frac{2\pi}{\hbar} V_{DA}^2 \frac{1}{\sqrt{4\pi\lambda k_B T}} \exp\left[-\left(\Delta G + \lambda\right)^2 / 4\pi\lambda k_B T\right] \qquad (1)$$

ΔG is the reaction free energy (difference between diabatic energies of the final and initial states) and λ the reorganization energy. For consistency with our previous study, the diabatic

energies and coupling parameters are derived from the ab initio data using the GMH method[45-46] by means of a unitary transformation from adiabatic to diabatic states:

$$\mathbf{U}^{\mathrm{T}}\mathbf{E}\mathbf{U} = \mathbf{H} \qquad (2)$$

E is the diagonal matrix of the adiabatic energy, and **U** the unitary matrix that diagonalizes the adiabatic dipole moment matrix $\mathbf{M}_{\mathrm{ad}}$:

$$\mathbf{U}^{\mathrm{T}}\mathbf{M}_{\mathrm{ad}}\mathbf{U} = \mathbf{M}_{\mathrm{d}} \qquad (3)$$

The diagonal elements of $\mathbf{M}_{\mathrm{ad}}$ correspond to the dipole moments of the adiabatic states, and the off-diagonal elements to the transition dipole moments. All elements are obtained as projections of the calculated dipole moments onto the vector connecting the centers of mass of the donor and acceptor sites. In the three-state treatment proposed by Cave and co-workers,[46] a block-diagonal matrix **H** is constructed where the couplings between the two states where the charge is on the same unit (GS and ES in the present case) is set to zero:

$$\mathbf{H}_{\mathrm{qd}} = \begin{pmatrix} \varepsilon_{\mathrm{GS}} & V_{\mathrm{GS\text{-}CT}} & 0 \\ V_{\mathrm{GS\text{-}CT}} & \varepsilon_{\mathrm{CT}} & V_{\mathrm{ES\text{-}CT}} \\ 0 & V_{\mathrm{ES\text{-}CT}} & \varepsilon_{\mathrm{ES}} \end{pmatrix} \qquad (4)$$

In this scheme, the adiabatic states at large donor-acceptor distances become equivalent to the diabatic states. In the MS-CASPT2 case, the elements of **E** are the energies of the three lowest adiabatic states, and the elements of $\mathbf{M}_{\mathrm{ad}}$ are obtained from the PM-CASCI wave function.

In the DFT treatment based on Kohn-Sham orbitals, the elements of **E** were approximated by the energies of the three highest occupied molecular π orbitals (π HOMOs) of the neutral system G-Ind. In turn, the dipole moments (elements of $\mathbf{M}_{\mathrm{ad}}$) are approximated as $\mu_{ij} = \langle \varphi_i | \hat{\mu} | \varphi_j \rangle$ where $\hat{\mu}$ is the dipole moment operator and φ_i and φ_j are the molecular orbitals. In our system, the orbitals of interest usually correspond to HOMO, HOMO-1 and HOMO-2. To illustrate this

point, the relevant orbitals for the π2 and T1 complexes are shown in Figure 2. In any case, a preliminary analysis of the Kohn-Sham orbitals of the system is required to confirm that the orbitals of interest actually correspond to the HOMOs. Some useful criteria to recognize the most important states are described in the literature (see for instance Refs. [15,45]).

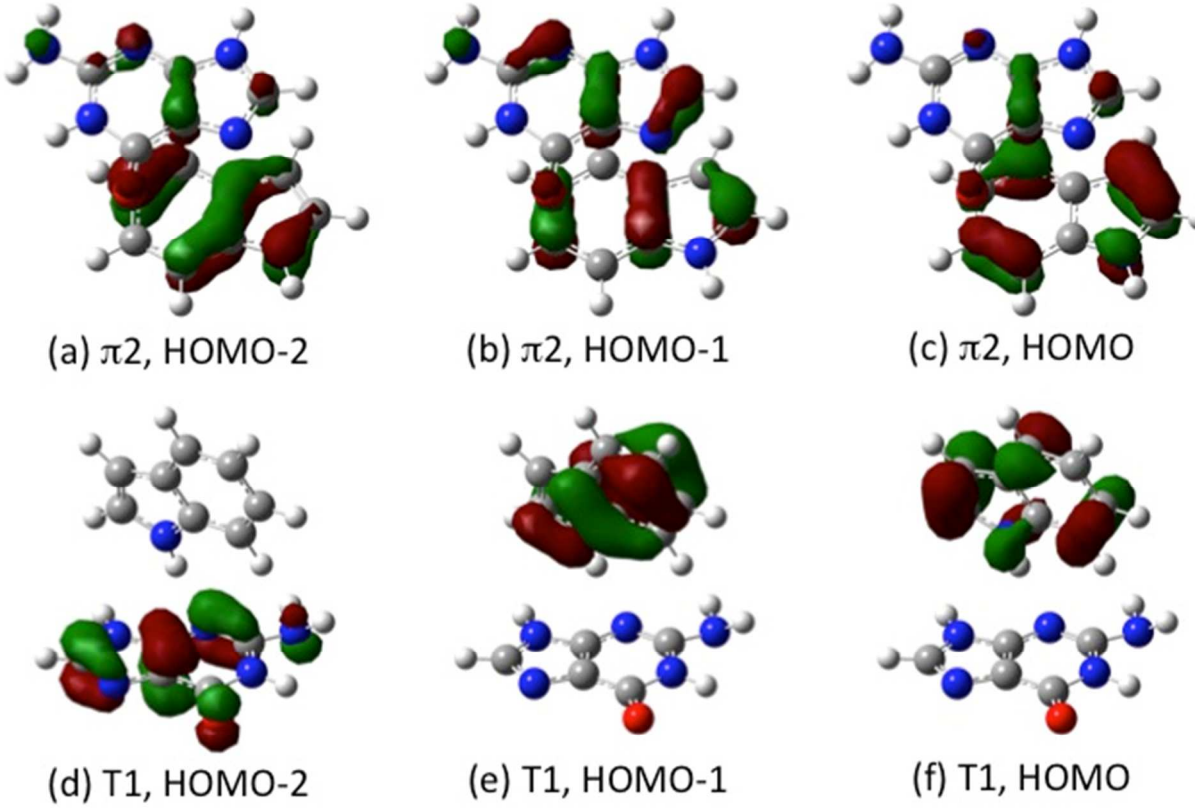

Figure 2. Isodensity plot at 0.05 density of the Kohn-Sham orbitals for complexes π2 (a - c) and T1 (d - f), calculated with CAM-B3LYP/6-31G*.

We note that the electronic coupling for hole (or excess electron) transfer between donor and acceptor can be estimated using HOMOs (or LUMOs in the excess electron case) stemming from quantum chemical calculations of isolated molecules.[47] This fragment orbital (FO) scheme was

used in combination with semiempirical, HF or DFT calculations to estimate the coupling (see eg Refs. [16,22-23,47] and references therein). Comparison of the matrix elements calculated with the GMH and FO schemes shows that both methods provide similar results (see the supporting material of Ref. [16]). Recently, the different FO schemes and their physical background were considered in detail.[21]

Another point to be mentioned is the overdelocalization of the electronic density in radical cations and anions predicted by unrestricted DFT calculations because of the self-interaction error. It was shown that despite this failure for the whole charge density computed for the radicals, the excess charge distribution in these species is properly described by the Kohn-Sham orbitals stemming from the DFT calculations of the corresponding neutral species.[26-27]

Results and Discussion

The parameters calculated for the 9 conformers with the 10 functionals under consideration, together with the MS-CASPT2 results and the results obtained with the Hartree-Fock (HF) orbitals, are displayed in Figures 3 - 7. The benchmark MS-CASPT2 parameters and the CAM-B3LYP results, which are representative for the Kohn-Sham based parameters, are also presented in Table 1. The complete set of data for the remaining functionals is provided in the Supporting Information, together with a statistical summary on the correlation between the orbital-based parameters and the benchmark ones. We start discussing the performance of the different DFT schemes and then consider the implications of the results for the three-state model.

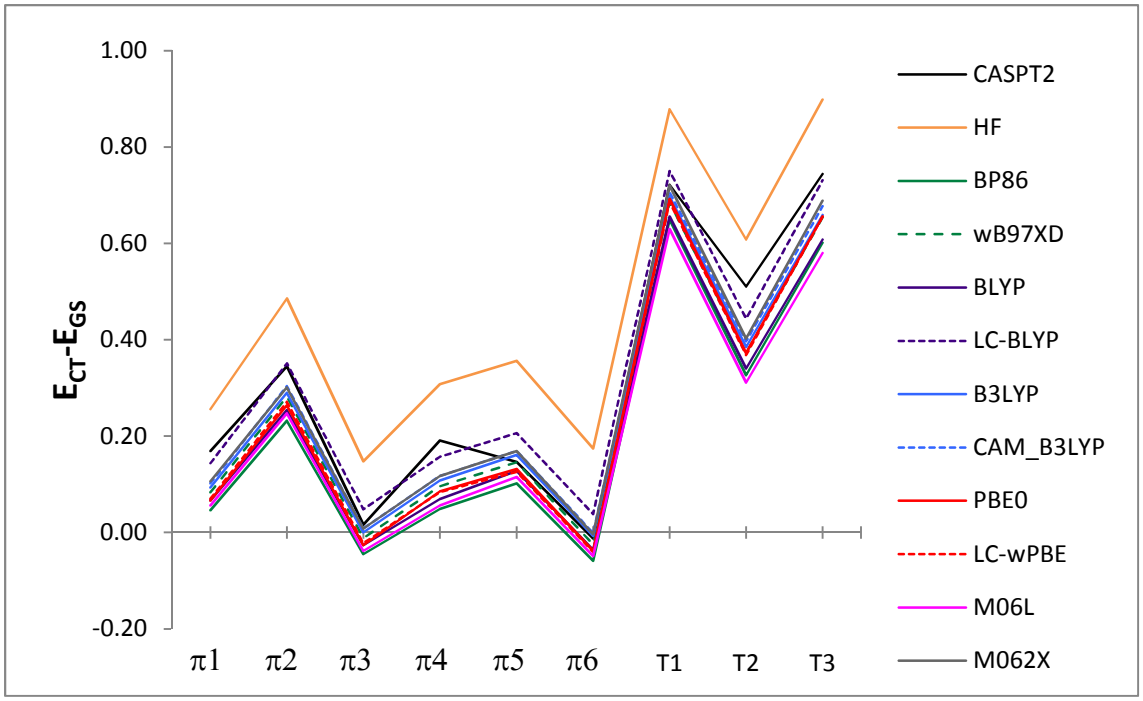

Figure 3. The energy of the charge shift $[Ind_1^+ G] \rightarrow [Ind\ G^+]$, $\varepsilon_{CT} - \varepsilon_{GS}$ (eV).

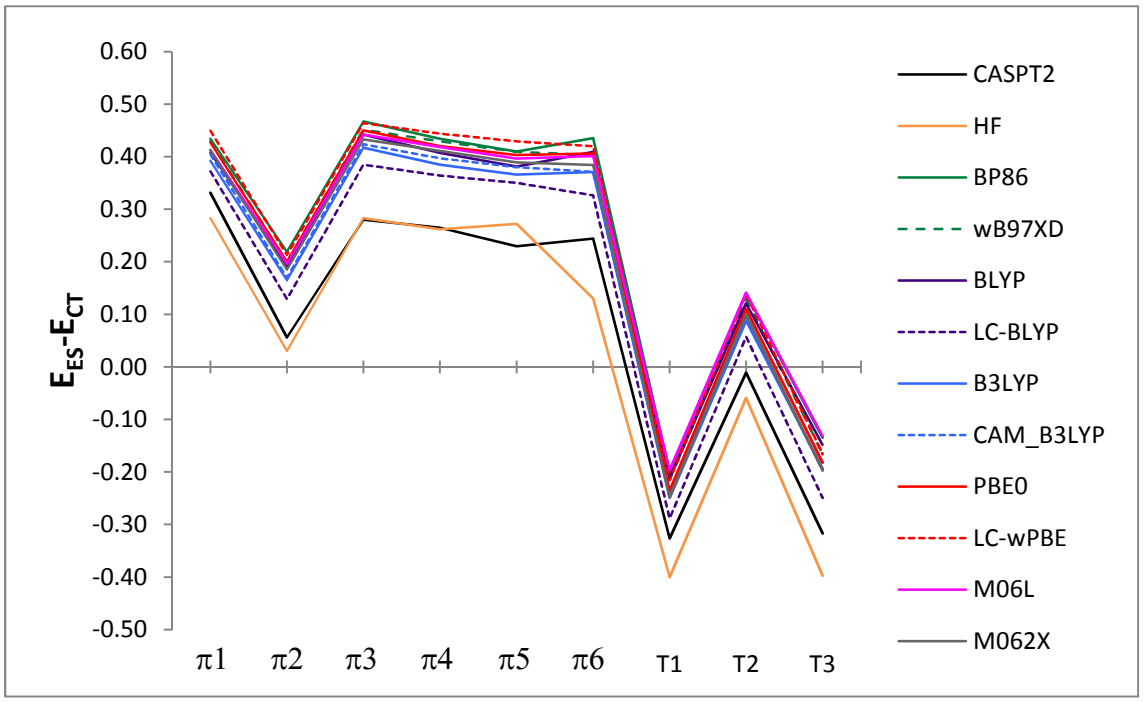

Figure 4. The energy of photoinduced charge shift $[Ind\ G^+] \rightarrow [Ind_2^+ G]$, $\varepsilon_{ES} - \varepsilon_{CT}$ (eV).

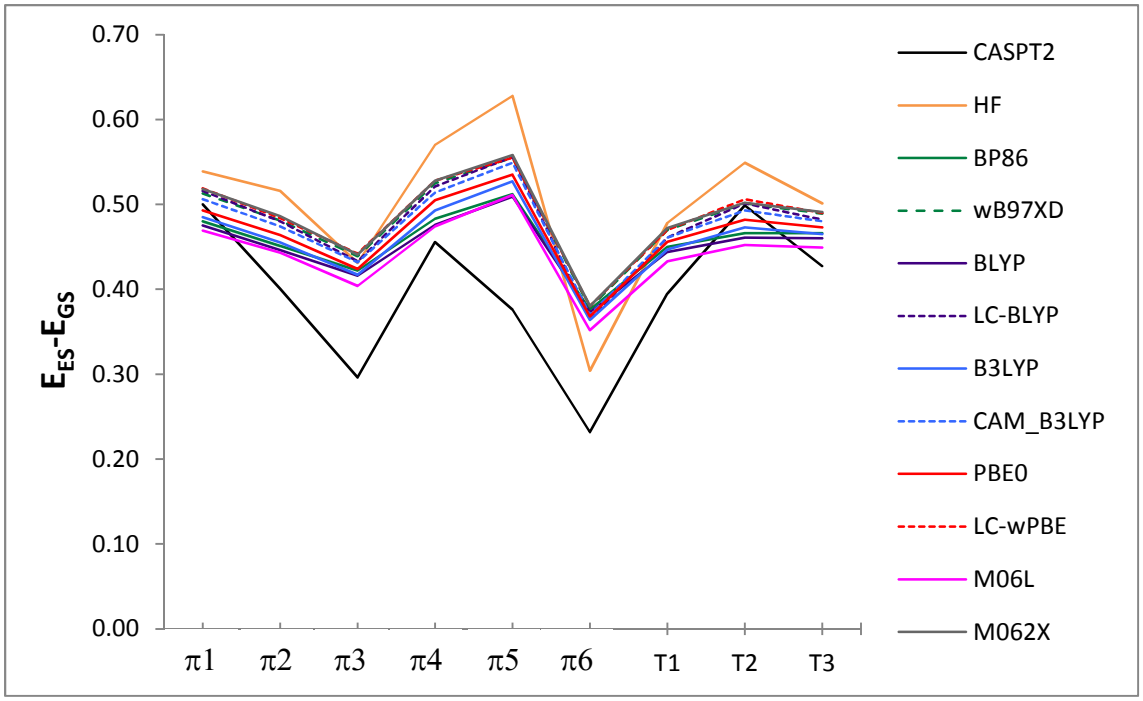

Figure 5. Diabatic $Ind_1^+ \rightarrow Ind_2^+$ excitation free energy, $\varepsilon_{ES} - \varepsilon_{GS}$ (eV).

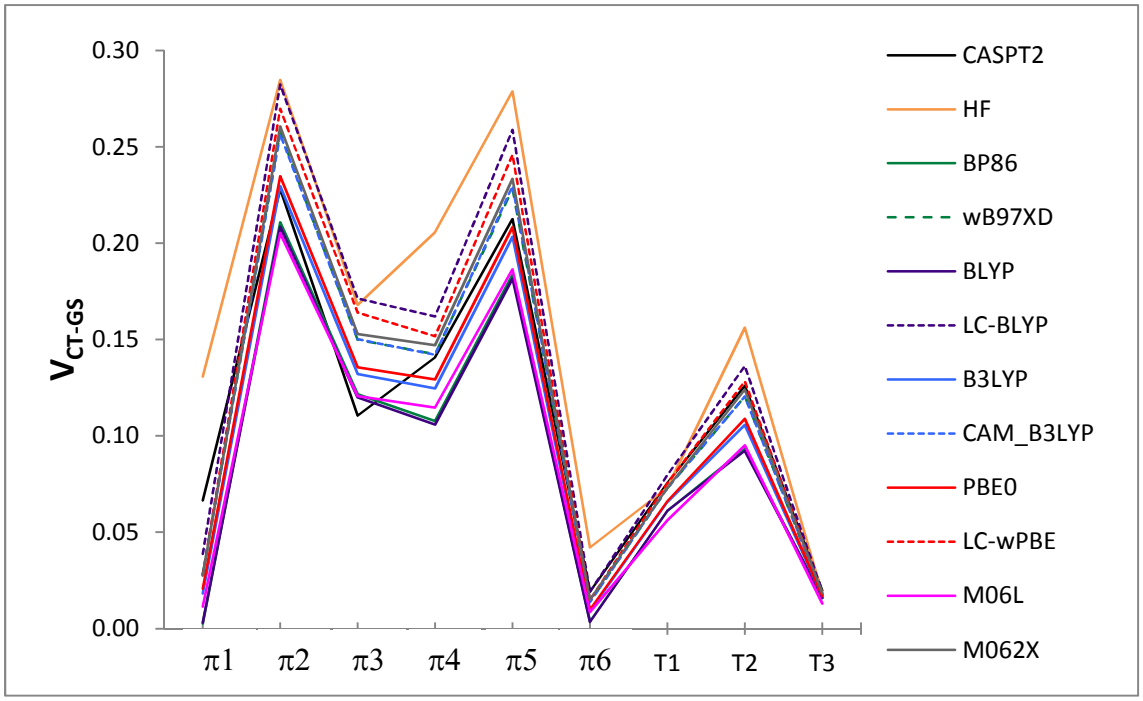

Figure 6. Coupling elements for charge recombination, V_{CT-GS}. (eV)

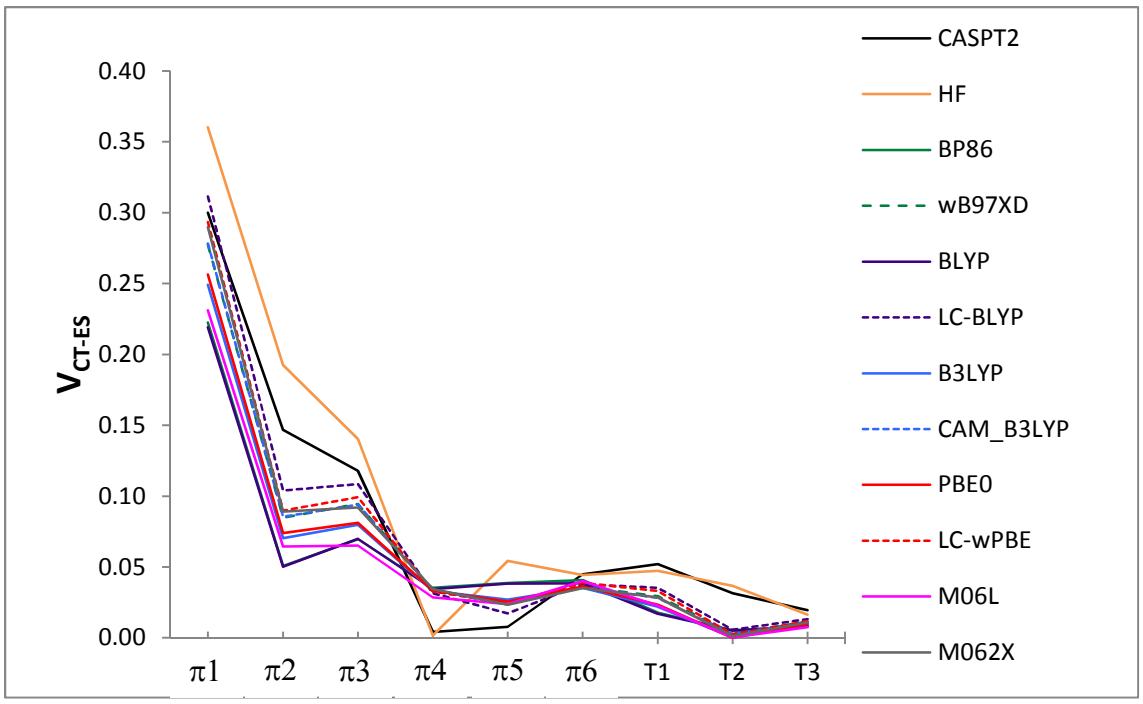

Figure 7. Coupling element for the photoinduced charge shift V_{CT-ES}, (eV).

Orbital-based calculation of HT parameters. Figures 3-5 and 6-7 display the relative diabatic energies and coupling elements, respectively, for the 9 conformers, calculated with all methods. The lines do not represent a physical correlation but serve as a guide to the eye. The black line shows the benchmark MS-CASPT2 results, the orange line the HF-based results, and the remaining lines the 10 functionals used in our study. The LC functionals are presented with dashed lines. The results show that there is a good correlation between the orbital-based parameters and the MS-CASPT2 benchmarks for all parameters of interest. The relative diabatic energies and couplings for the 9 complexes span a range of about 0.8 eV and 0.3 eV, respectively (see also Table 1), and the orbital-based values follow closely the variations between the different conformations at the MS-CASPT2 level. In general, the difference between the diabatic energies of the G^+ and Ind_1^+ states, $\varepsilon_{CT} - \varepsilon_{GS}$, is underestimated by the Kohn-Sham orbital based

approach by 0.1-0.2 eV with respect to the reference values (Figure 3). Looking closer at the ε_{CT} - ε_{GS} parameter, which corresponds to the charge shift energy from G^+ to Ind_1^+, there are some small differences between MS-CASPT2 and the Kohn-Sham approach. For instance, MS-CASPT2 gives that the charge shift energy for the π4 complex is greater than for the π5 one, but the Kohn-Sham approach gives the opposite trend. This occurs because the difference between the charge shift energies of the two complexes, at the MS-CASPT2 level, is small (0.045 eV). However, the Kohn-Sham approach gives a correct estimation of the charge shift parameter of π4 and π5 within 0.1 eV. The HF-based energies follow the opposite trend than the Kohn-Sham based ones and overestimate the MS-CASPT2 values. In turn, the relative energy of the CT state with respect to the Ind_2^+ state, ε_{ES}-ε_{CT}, is overestimated with the Kohn-Sham approach by 0.1-0.2 eV, compared to MS-CASPT2 (Figure 4). In this case, the agreement of the HF values with MS-CASPT2 is better. The orbital-based approach also gives a good estimate of the adiabatic excitation energy of the charged Ind^+ molecule. In general, the MS-CASPT2 values are somewhat overestimated, by up to 0.2 eV, and the DFT values are in better agreement with MS-CASPT2 than the HF ones.

Turning to the coupling elements (Figure 6), the differences between the DFT and the MS-CASPT2 results are less consistent than those found for the energies. The DFT couplings values $V_{GS\text{-}CT}$ and $V_{ES\text{-}CT}$ are overestimated in some conformations but underestimated in others. As to the HF parameters, both the $V_{GS\text{-}CT}$ and $V_{ES\text{-}CT}$ couplings are somewhat overestimated.

A further assessment of the performance of the considered methods for the calculation of the coupling elements is given in Table SI1 (Supporting Information), which shows the differences between the orbital-based couplings and the MS-CASPT2 benchmarks. The RMSD column shows the root mean square of the difference between the orbital-based coupling and the MS-

CASPT2 values for each functional and HF. In addition, we fitted the orbital-based couplings to the reference data and present the square of the correlation coefficient (R^2), together with the slope and the y-intercept of the fit. In most cases, there is a good correlation, $R^2 > 0.9$. The results are presented in increasing order of error, taken as the average RMSD for the V_{GS-CT} and V_{ES-CT} couplings. Overall, the DFT schemes work better than the HF method. The best results are obtained for seven functionals (CAM-B3LYP, ωB97XD, M062X, LC-BLYP, LC-ωPBE, PBE0 and B3LYP) where the average RMSD lies between 0.025 and 0.030 eV. The average error for the remaining four methods (M06L, HF, BP86 and BLYP) is slightly larger, up to 0.040 eV. For the seven best functionals, the trend is to overestimate the GS-CT couplings and underestimate the ES-CT couplings (correlation slope larger and smaller than 1, respectively), which agrees with the trends shown in Figures 6 and 7. Moreover, the inclusion of a long-range correction to avoid self-interaction errors helps to improve the RMSD, since the four long-range corrected functionals (CAM-B3LYP, ωB97XD, LC-BLYP, LC-ωPBE) are among the five with the smallest average RMSD. Comparison of the B3LYP and PBE0 data with the CAM-B3LYP and LC-ωPBE ones, respectively, also shows that the long-range correction improves the ES-CT couplings more significantly than the GS-CT ones.

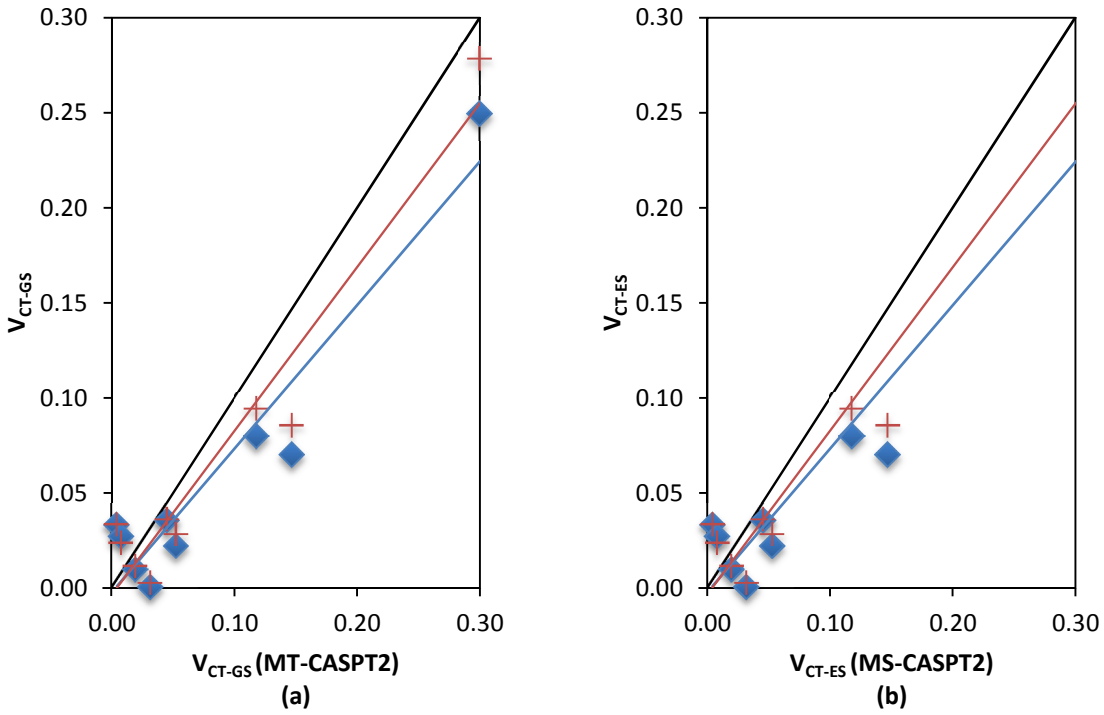

Figure 8. Linear regression fits of the orbital-based couplings with respect to MS-CASPT2 for the CAM-B3LYP (red) and B3LYP (blue) functionals. (a) V_{CT-GS} and (b) V_{CT-ES}. The diagonal black line represents the ideal correlation.

A more detailed look at the individual results for the best functional of our study, CAM-B3LYP, together with the B3LYP counterpart, is given in Figure 8, where we plot the values of the DFT-based couplings on the y-axis with respect to the MS-CASPT2 couplings on the x-axis. As noted previously, the DFT-based V_{GS-CT} couplings are slightly overestimated with respect to MS-CASPT2, whereas the V_{ES-CT} ones are underestimated. It is also clear from Figure 8 that the three methods give couplings within the same order of magnitude for all conformers. At the same time, while all couplings have similar absolute errors, the relative errors are more significant for the smaller couplings.

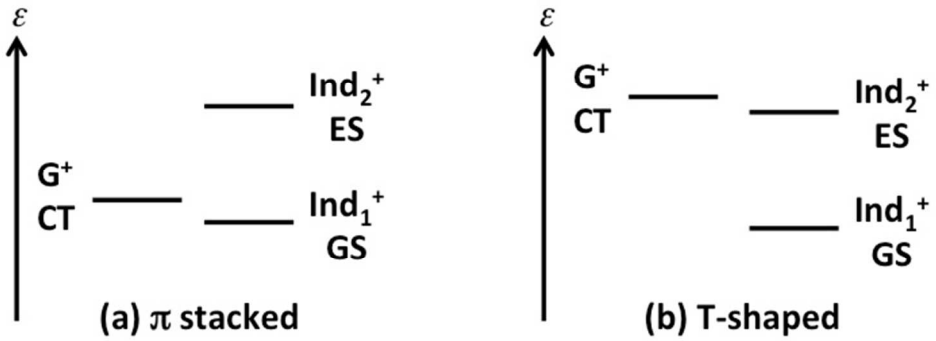

Figure 9. Approximate ordering of diabatic states for the (a) π stacked and (b) T-shaped conformations.

Importance of the three-state model. Our results also give new insights into the importance of the three-state model for handling HT in the G-Ind system. In our previous study with the three-state model we only considered the π stacked conformers π1-π6,[15] and here we have included three T-shaped conformers. According to Figures 3 and 4, the MS-CASPT2 energy ε_{CT} of the G^+ state for the π stacked conformers π1-π5 lies in between the energies of the indole states, ε_{GS} and ε_{ES}, since the values of ε_{CT} - ε_{GS} and ε_{ES} - ε_{CT} are positive. This situation is shown graphically in Figure 9a. In contrast to this, in the T-shaped conformers the G^+ state is similar or higher in energy than the Ind_2^+ state, as shown by the negative values of ε_{ES} - ε_{CT} in Figure 4. Thus, the energy diagram for the T-shaped conformers resembles the situation of Figure 9b. The change in the energy order of the diabatic states can also be recognized from the shapes of the adiabatic Kohn-Sham orbitals, which are shown exemplarily for the π2 and T1 complexes in Figure 2. In the π2 case, the orbital with the highest contribution from the guanine fragment is the HOMO-1, whereas in the T1 case it is the HOMO-2. This change in the energy order is a

consequence of the geometric arrangement shown in Figure 1. The π orbitals of G interact with some of the Ind hydrogen atoms, which induces a lowering of the π orbital energy so that the G oxidation potential, ie the ε_{CT} energy, is increased. This suggests that the Ind^+ excited state may be specially relevant role in T-shaped conformations of the G-Ind complex.

Conclusions

The dynamics of hole transfer from DNA to protein (e.g. in nucleosome core particles) are critically dependent on the relative energy and coupling matrix element of the final and initial state of the electron transfer reaction. The most relevant pair of the hole donor and the hole acceptor in such systems are guanine and tryptophan (indole), the species which have the lowest ionization potential among nucleobases and amino acid residues, respectively. Using the MS-CASPT2 method, we have estimated the ET parameters for 9 different structures including π-stacked and T-shape configurations of the G-Ind complex. Because there is only a small gap between the ground and excited state energies, the 2-state treatment cannot be applied to the system and the three-state model has been employed (specially in the case of T-shaped conformations). The obtained data have been used to estimate the performance of the approximate scheme based on the Kohn-Sham orbitals stemming from DFT calculations with different exchange-correlation functionals. Our results suggest that this simple DFT approach gives good estimates for all ET parameters, better than those obtained with the HF orbitals. The scheme is robust and the quality of the obtained data is not very sensitive to the type of the functional. Inclusion of the long-range correction improves the accuracy of predicted couplings. The most accurate data have been obtained with the CAM-B3LYP method.

Our results imply that the scheme can also be used to estimate excited state properties of radical cation systems and interpret spectroscopic measurements for transient species. Because of its accuracy and low computational cost, the Kohn-Sham orbital model also allows one to calculate relatively large models and account for the effects of structural fluctuations on the ET process. The sensitivity of the HT energetics in G-Ind to structural changes suggests that fluctuations in the arrangement of the donor and acceptor may even change the sign of the driving force and thereby switch the direction of HT. The tabulated MS-CASPT2 results may also be used to evaluate the performance of other computational strategies when modeling hole transfer in DNA-protein complexes.

Acknowledgments. This work has been supported by grants CTQ2011-23441 and CTQ2011-26573 from the Spanish Ministerio de Economía y Competividad (MINECO), SGR0528 from the Catalan Agència de Gestió d'Ajuts Universitaris i de Recerca (AGAUR), UNGI08-4E-003 and UNGI10-4E-801 from MINECO and the European Fund for Regional Development (FEDER), and the Xarxa de Referència en Química Teòrica i Computacional de Catalunya from AGAUR.

Supporting Information. Structures (S1), statistical analysis (Table S2), calculated parameters (Tables S3-S11), structures (Figure S1) and Cartesian coordinates of all structures. This material is available free of charge via the Internet at http://pubs.acs.org.

References

(1) Berlin, Y. A.; Kurnikov, I. V.; Beratan, D.; Ratner, M. A.; Burin, A. L. In *Long-Range Charge Transfer in DNA II*, 2004; Vol. 237.
(2) Genereux, J. C.; Barton, J. K., *Chem. Rev.*, 2010, **110**, 1642-1662.
(3) *Long-Range Charge Transfer in DNA*; Schuster, G. B., Ed.; Springer: Berlin, 2004; Vol. 236.
(4) Siriwong, K.; Voityuk, A. A., *WIREs Comput. Mol. Sci.*, 2012, **2**, 780-794.
(5) Venkatramani, R.; Keinan, S.; Balaeff, A.; Beratan, D. N., *Coord. Chem. Rev.*, 2011, **255**, 635-648.
(6) Sancar, A., *Chem. Rev.*, 2003, **103**, 2203-2237.
(7) Bjorklund, C. C.; Davis, W. B., *Nucleic Acids Res.*, 2006, **34**, 1836-1846.
(8) Milligan, J. R.; Aguilera, J. A.; Ly, A.; Tran, N. Q.; Hoang, O.; Ward, J. F., *Nucleic Acids Res.*, 2003, **31**, 6258-6263.
(9) Dumont, A.; Zheng, Y.; Hunting, D.; Sanche, L., *J. Chem. Phys.*, 2010, **132**.
(10) Milligan, J. R.; Tran, N. Q.; Ly, A.; Ward, J. F., *Biochemistry*, 2004, **43**, 5102-5108.
(11) Voityuk, A. A.; Davis, W. B., *J. Phys. Chem. B*, 2007, **111**, 2976-2985.
(12) Wagenknecht, H. A.; Rajski, S. R.; Pascaly, M.; Stemp, E. D. A.; Barton, J. K., *J. Am. Chem. Soc.*, 2001, **123**, 4400-4407.
(13) Wagenknecht, H. A.; Stemp, E. D. A.; Barton, J. K., *J. Am. Chem. Soc.*, 2000, **122**, 1-7.
(14) Cullis, P. M.; Jones, G. D. D.; Symons, M. C. R.; Lea, J. S., *Nature*, 1987, **330**, 773-774.
(15) Butchosa, C.; Simon, S.; Blancafort, L.; Voityuk, A., *J. Phys. Chem. B*, 2012, **116**, 7815-7820.
(16) Butchosa, C.; Simon, S.; Voityuk, A. A., *Org. Biomol. Chem.*, 2010, **8**, 1870-1875.
(17) Butchosa, C.; Simon, S.; Voityuk, A. A., *Comput. Theor. Chem.*, 2011, **975**, 38-41.
(18) Butchosa, C.; Simon, S.; Voityuk, A. A., *Int. J. Quantum Chem*, 2012, **112**, 1838-1843.
(19) Jena, N. R.; Mishra, P. C.; Suhai, S., *J. Phys. Chem. B*, 2009, **113**, 5633-5644.
(20) Zhao, J.; Yang, H.; Zhang, M.; Bu, Y., *ChemPhysChem*, 2013, **14**, 1031-1042.
(21) Kubas, A.; Hoffmann, F.; Heck, A.; Oberhofer, H.; Elstner, M.; Blumberger, J., *J. Chem. Phys.*, 2014, **140**, 104105.
(22) Kubar, T.; Elstner, M., *J. Phys. Chem. B*, 2010, **114**, 11221-11240.
(23) Kubar, T.; Elstner, M., *Phys. Chem. Chem. Phys.*, 2013, **15**, 5794-5813.
(24) Pavanello, M.; Neugebauer, J., *J. Chem. Phys.*, 2011, **135**.
(25) Sini, G.; Sears, J. S.; Bredas, J.-L., *J. Chem. Theory Comput.*, 2011, **7**, 602-609.
(26) Felix, M.; Voityuk, A. A., *J. Phys. Chem. A*, 2008, **112**, 9043-9049.
(27) Felix, M.; Voityuk, A. A., *Int. J. Quantum Chem*, 2011, **111**, 191-201.
(28) Finley, J.; Malmqvist, P. A.; Roos, B. O.; Serrano-Andres, L., *Chem. Phys. Lett.*, 1998, **288**, 299-306.
(29) Roos, B. O.; Andersson, K., *Chem. Phys. Lett.*, 1995, **245**, 215-223.
(30) Becke, A. D., *Phys. Rev. A*, 1988, **38**, 3098-3100.
(31) Perdew, J. P., *Phys. Rev. B*, 1986, **33**, 8822-8824.
(32) Lee, C. T.; Yang, W. T.; Parr, R. G., *Phys. Rev. B*, 1988, **37**, 785-789.
(33) Becke, A. D., *J. Chem. Phys.*, 1993, **98**, 5648-5652.
(34) Perdew, J. P.; Emzerhof, M.; Burke, K., *J. Chem. Phys.*, 1996, **105**, 9982-9985.
(35) http://www.marcelswart.eu/dft-poll, accessed on Apr 23, 2014.
(36) Zhao, Y.; Truhlar, D. G., *Theor. Chem. Acc.*, 2008, **120**, 215-241.

(37) Dreuw, A.; Head-Gordon, M., *J. Am. Chem. Soc.*, 2004, **126**, 4007-4016.
(38) Dreuw, A.; Weisman, J. L.; Head-Gordon, M., *J. Chem. Phys.*, 2003, **119**, 2943-2946.
(39) Perdew, J. P.; Parr, R. G.; Levy, M.; Balduz, J. L., *Phys. Rev. Lett.*, 1982, **49**, 1691-1694.
(40) Zhang, Y. K.; Yang, W. T., *J. Chem. Phys.*, 1998, **109**, 2604-2608.
(41) Song, J.-W.; Hirosawa, T.; Tsuneda, T.; Hirao, K., *J. Chem. Phys.*, 2007, **126**.
(42) Yanai, T.; Tew, D. P.; Handy, N. C., *Chem. Phys. Lett.*, 2004, **393**, 51-57.
(43) Chai, J.-D.; Head-Gordon, M., *Phys. Chem. Chem. Phys.*, 2008, **10**, 6615-6620.
(44) Iikura, H.; Tsuneda, T.; Yanai, T.; Hirao, K., *J. Chem. Phys.*, 2001, **115**, 3540-3544.
(45) Cave, R. J.; Newton, M. D., *J. Chem. Phys.*, 1997, **106**, 9213-9226.
(46) Rust, M.; Lappe, J.; Cave, R. J., *J. Phys. Chem. A*, 2002, **106**, 3930-3940.
(47) Newton, M. D., *Chem. Rev.*, 1991, **91**, 767-792.

Table 1. Calculated ET parameters (diabatic free energies and couplings) for the 9 conformers with the MS-CASPT2 and CAM-B3LYP methods.

Parameter	Method	π1	π2	π3	π4	π5	π6	T1	T2	T3
ε_{CT} - ε_{GS}	MS-CASPT2	0.169	0.345	0.016	0.191	0.146	-0.012	0.722	0.510	0.744
	CAM-B3LYP	0.102	0.304	0.008	0.117	0.169	-0.001	0.706	0.397	0.677
ε_{ES} - ε_{CT}	MS-CASPT2	0.331	0.056	0.280	0.265	0.230	0.244	-0.327	-0.011	-0.317
	CAM-B3LYP	0.404	0.170	0.424	0.397	0.380	0.371	-0.245	0.096	-0.197
ε_{ES} - ε_{GS}	MS-CASPT2	0.500	0.401	0.296	0.455	0.376	0.232	0.395	0.499	0.427
	CAM-B3LYP	0.506	0.474	0.432	0.514	0.549	0.370	0.461	0.493	0.480
V_{CT-GS}	MS-CASPT2	0.301	0.147	0.118	0.004	0.008	0.045	0.052	0.032	0.020
	CAM-B3LYP	0.278	0.085	0.094	0.033	0.024	0.036	0.028	0.003	0.011
V_{CT-ES}	MS-CASPT2	0.067	0.228	0.110	0.141	0.212	0.019	0.076	0.126	0.020
	CAM-B3LYP	0.028	0.256	0.150	0.142	0.230	0.014	0.073	0.120	0.018

TOC

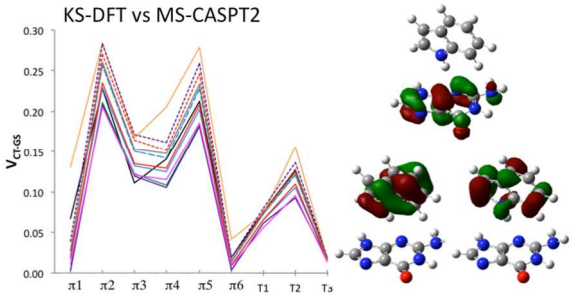

The electron transfer parameters for the 3-state G···Ind system can be obtained with an efficient Kohn-Sham orbital based scheme.